Collisional energy loss in a finite size QCD matter

Magdalena Djordjevic
Department of Physics, Ohio State University, 191 West Woodruff Avenue, Columbus, Ohio 43210, USA
(Received 10 May 2006; published 15 December 2006)

Computation of collisional energy loss in a finite size QCD medium has become crucial to obtain reliable predictions for jet quenching in ultrarelativistic heavy ion collisions. We here compute this energy loss up to the zeroth order in opacity. Our approach consistently treats both soft and hard contributions to the collisional energy loss. Consequently, it removes the unphysical energy gain in a region of lower momenta obtained by previous computations. Most importantly, we show that for characteristic QCD medium scales, finite size effects on the collisional energy loss are not significant.

DOI: 10.1103/PhysRevC.74.064907 PACS number(s): 12.38.Mh, 24.85.+p, 25.75.−q

I. INTRODUCTION

The suppression pattern of high transverse momentum hadrons is a powerful tool to map out the density of a QCD plasma created in ultrarelativistic heavy ion collisions (URHIC) [1–3]. This suppression (called jet quenching) is considered to be mainly a consequence of medium induced radiative energy loss of high energy partons [4–7]. However, recent nonphotonic single electron data [8,9] (which present an indirect probe of heavy quark energy loss) showed large disagreement with the radiative energy loss predictions, as long as realistic values of parameters are assumed [10]. This raised the question of what is the cause for the observed discrepancy.

Recent studies [11,12] suggested that one of the basic assumptions that pQCD collisional energy loss is negligible compared to radiative [13] may be incorrect. In [11] it was shown that, for a range of parameters relevant for RHIC, radiative and collisional energy losses for heavy quarks were in fact comparable to each other, and therefore collisional energy loss can not be neglected in the computation of jet quenching. This result came as a surprise because from the earlier estimates [13–18], the typical collisional energy loss was erroneously considered to be small compared to the radiative energy loss. In [19] it was consequently suggested that the inclusion of collisional energy loss may help in solving the "single electron puzzle." However, in that study (as well as [11–18]) finite size effects were not taken into account.

A recent paper by Peigne *et al.* [20] is the first study that made an attempt to include finite size effects in the collisional energy loss. This work suggested that collisional energy loss is large only in the ideal infinite medium case, while finite size effects lead to a significant reduction of the collisional energy loss. However, this paper did not completely separate collisional and radiative energy loss effects. Consequently, it remained unclear how important are the finite size effects on the collisional energy loss.

Therefore, it became necessary to consistently compute (only) the collisional energy loss in finite size QCD medium. Additionally, this paper aims to address whether—and to what extent—there is an over-counting between collisional and radiative energy loss computations.

The outline of the paper is as follows. In Sec. II, we will compute the collisional energy loss in a finite size QCD medium. In Sec. III, we will consider the special case when a particle is produced at $x_0 = -\infty$ (infinite medium case). We will show that in special limits, our calculations recover previous results [14,15]. However, contrary to Refs. [14,15], our computation does not encounter unphysical energy gain in the low momentum region [14,15]. In Sec. IV we will give a numerical study of the collisional energy loss in both finite and infinite QCD medium. Contrary to the results obtained in Peigne *et al.* [20] we will show that finite size effects do not have a significant effect on the collisional energy loss. The conclusions and outlook are given in Sec. V.

II. COLLISIONAL ENERGY LOSS IN FINITE SIZE QCD MEDIUM

In this section we will compute the collisional energy loss (up to the zeroth order in opacity) when the jet is produced in a finite size dielectric medium. The contribution to this energy loss comes from one Hard-Thermal Loop (HTL) gluon propagator (see Appendix A), which is the reason why we call it the zeroth order in opacity collisional energy loss (note the analogy with the zeroth order in opacity radiative energy loss [21–23], which is further discussed in Appendix A).

In this computation we use the most intuitive approach, i.e., we compute the diagram $|M_{el}|$ shown in Fig. 1. Note that the "blob" represents the effective gluon propagator. A proof of the validity of this approach is given in Appendix A. This approach has already been used without proof in Refs. [24,25], under the justification that it reproduces the same results as the imaginary time formalism.

Similar to Ref. [23] we introduce the finite size medium by starting from the approach described in Ref. [26]. We consider a static medium of size L, and assume that collisional energy loss can occur only inside the medium. The Feynman diagram $|M_{el}|$ (see Fig. 1) then represents the source J, which at time x_0 produces an off-shell jet with momentum p, and subsequently (at $x_1 > x_0$) exchanges a virtual gluon with parton in the medium with momentum k. The jet and the medium parton emerge with momentum p' and k' respectively. Since our focus is on heavy quark jets with mass M, we here neglect the thermal shifts of the heavy quark mass.

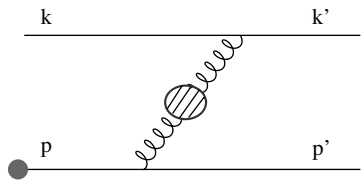

FIG. 1. Feynman diagram for the amplitude that contributes to the collisional energy loss in QCD medium. The large dashed circle ("blob") represents the effective gluon propagator [21].

We assume, as in Ref. [27], that source J changes slowly with p', i.e. that $\tilde{J}(p'+q) \approx \tilde{J}(p)$[1]. Since we consider both soft and hard contributions, we take into account spin effects. The computation that we present in this paper is gauge invariant [24], but for simplicity we further use Coulomb gauge.

The effective gluon propagator shown in Fig. 1 has both transverse and longitudinal contributions [28–32]. In Coulomb gauge the gluon propagator has the following form:

$$D^{\mu\nu}(\omega,\vec{\mathbf{q}}) = -P^{\mu\nu}\Delta_T(\omega,\vec{\mathbf{q}}) - Q^{\mu\nu}\Delta_L(\omega,\vec{\mathbf{q}}), \tag{1}$$

where $q = (\omega,\vec{\mathbf{q}})$ is the four-momentum of the gluon, while Δ_T and Δ_L are effective transverse and longitudinal gluon propagators given by [32]

$$\Delta_T^{-1} = \omega^2 - \vec{\mathbf{q}}^2 - \frac{\mu^2}{2} - \frac{(\omega^2-\vec{\mathbf{q}}^2)\mu^2}{2\vec{\mathbf{q}}^2} \times \left(1 + \frac{\omega}{2|\vec{\mathbf{q}}|}\ln\left|\frac{\omega-|\vec{\mathbf{q}}|}{\omega+|\vec{\mathbf{q}}|}\right|\right), \tag{2}$$

$$\Delta_L^{-1} = \vec{\mathbf{q}}^2 + \mu^2\left(1 + \frac{\omega}{2|\vec{\mathbf{q}}|}\ln\left|\frac{\omega-|\vec{\mathbf{q}}|}{\omega+|\vec{\mathbf{q}}|}\right|\right), \tag{3}$$

where $\mu_D^2 = g^2T^2(1+\frac{N_f}{6})$ is the Debye mass.

The only nonzero terms in transverse ($P_{\mu\nu}$) and longitudinal ($Q_{\mu\nu}$) projectors are the following:

$$P^{ij} = \delta^{ij} - \frac{q^i q^j}{|\vec{\mathbf{q}}|^2}, \tag{4}$$

$$Q^{00} = 1. \tag{5}$$

The matrix element for this 0^{th} order in opacity collisional process can then be written in the following form (for simplicity we here omit color factors, whose contribution we will add in the end):

$$\begin{aligned} iM_{el} = &\int d^4x_0\ J(x_0)\ d^4x_1\ (-i)\int\frac{d^3\vec{\mathbf{p}}}{(2\pi)^3 2E}\ \Theta(t_1-t_0) \\ &\times\Theta(L/v-(t_1-t_0))\bar{u}(p',s')e^{ip'x_1}\ ig\gamma^\mu\ u(p,s) \\ &\times e^{-ipx_1}\int d^4x_2\ (-i)\int\frac{d^4q}{(2\pi)^4}D_{\mu\nu}(q)e^{-iq(x_2-x_1)} \\ &\times\bar{u}(k',\lambda')e^{ik'x_2}\ ig\gamma^\nu\ u(k,\lambda)e^{-ikx_2}. \end{aligned} \tag{6}$$

Here p, s, k, and λ are the four-momenta and spins of the incoming jet and medium parton, while the corresponding primed variables correspond to outgoing jet and medium parton (the medium parton can be quark, antiquark or gluon). The medium partons are considered to be massless, i.e., four-momentum k (k') is assumed to be $k = (|\vec{\mathbf{k}}|,\vec{\mathbf{k}})$ ($k' = (|\vec{\mathbf{k}}'|,\vec{\mathbf{k}}')$). The condition that the interaction between jet and medium parton has to occur inside the QCD medium of finite size L is implemented through the second θ function giving maximal interaction time of $(t_1-t_0)_{\max} = L/v$. We will further define $x \equiv x_1 - x_0 = (t,\vec{\mathbf{x}})$.

Equation (6) simplifies to

$$\begin{aligned} iM_{el} = &g^2\int\frac{d^3\vec{\mathbf{p}}}{(2\pi)^3 2E}\int\frac{d^4q}{(2\pi)^4}\int d^4x_0\ J(x_0)e^{i(p'+q)x_0} \\ &\times\int d^3\vec{\mathbf{x}}\int_0^{L/v}dt\ e^{-i(p-p'-q)x}(2\pi)^4\delta(k'-k-q) \\ &\times D_{\mu\nu}(q)\bar{u}(p',s')\gamma^\mu u(p,s)\bar{u}(k',\lambda')\gamma^\nu u(k,\lambda) \\ = &\tilde{J}(p')\ \frac{1}{2E}\frac{1-e^{-i(E-E'-\omega)L/v}}{E-E'-\omega}i\mathcal{M}, \end{aligned} \tag{7}$$

where $E = \sqrt{M^2+\vec{\mathbf{p}}^2}$, M is the jet mass, $\vec{\mathbf{p}} = \vec{\mathbf{p}}' - (\vec{\mathbf{k}}'-\vec{\mathbf{k}})$ and $\omega = |\vec{\mathbf{k}}'| - |\vec{\mathbf{k}}|$.

In the last step we used $\tilde{J}(p'+q) \approx \tilde{J}(p')$ [27] and defined

$$\mathcal{M} = g^2 D_{\mu\nu}(k'-k)\bar{u}(p',s')\gamma^\mu u(p,s)\bar{u}(k',\lambda')\gamma^\nu u(k,\lambda). \tag{8}$$

In this paper we consider the case of highly energetic jets, where $|\vec{\mathbf{q}}| \ll E$. In this limit E' becomes $E' \approx E - \vec{\mathbf{v}}\cdot\vec{\mathbf{q}}$. Here $\vec{\mathbf{v}}$ is the velocity of the initial jet, i.e., the jet four-momentum p is equal to $p = (\frac{M}{\sqrt{1-v^2}}, \frac{M\vec{\mathbf{v}}}{\sqrt{1-v^2}})$.

Further, the matrix element given in Eq. (7) has to be squared, averaged over initial spin s of the jet and summed over all other spins.

$$\frac{1}{2}\sum_{\text{spins}}|M_{el}|^2 = |\tilde{J}(p')|^2\frac{1}{E^2}\frac{\sin^2\left[(\omega-\vec{\mathbf{v}}\cdot\vec{\mathbf{q}})\frac{L}{2v}\right]}{(\omega-\vec{\mathbf{v}}\cdot\vec{\mathbf{q}})^2} \times\frac{1}{2}\sum_{\text{spins}}|\mathcal{M}|^2, \tag{9}$$

where $\frac{1}{2}\sum_{\text{spins}}|\mathcal{M}|^2$ is given in Appendix B.

The differential energy loss is equal to $dE_{el} = \omega\, d\Gamma_{el}$, where collisional interaction rate $d\Gamma_{el}$ can be extracted from Eq. (9) as (see Ref. [27])

$$d^3N_J\ d\Gamma_{el} \approx \frac{1}{2}\sum_{\text{spins}}|M_{el}|^2\frac{d^3\vec{\mathbf{p}}'}{(2\pi)^3 2E'}\frac{d^3\vec{\mathbf{k}}}{(2\pi)^3 2k}\frac{d^3\vec{\mathbf{k}}'}{(2\pi)^3 2k'} \times\sum_{\xi=q,\bar{q},g}n_{eq}^\xi(k)\left(1\pm n_{eq}^\xi(k')\right). \tag{10}$$

Here

$$d^3N_J = d_R|\tilde{J}(p')|^2\frac{d^3\vec{\mathbf{p}}'}{(2\pi)^3 2E'}, \tag{11}$$

and $d_R = 3$ (for three dimensional representation of the quarks). In Eq. (10), $n_{eq}^\xi(k)$ is the equilibrium momentum distribution at temperature T of the incoming parton ξ, where ξ denotes quark, antiquark or gluon. $(1\pm n_{eq}^\xi(k'))$ is a factor

[1]Note that the current in coordinate space is denoted with J, while the current in momentum space is denoted with $\tilde{J}$.

associated with the outgoing parton, where + corresponds to the gluon contribution, and − to (anti)quark contribution.

In this paper, we are interested only in the computation of the collisional energy loss. It is straightforward to show that in the collisional energy loss calculations, the $\pm n^{\xi}_{eq}(k')$ part in $(1 \pm n^{\xi}_{eq}(k'))$ can be dropped because the corresponding term in the energy loss integrand is odd under the exchange of $\vec{\mathbf{k}}$ and $\vec{\mathbf{k}}'$, and integrates to zero (see also Ref. [24]). Therefore, for the purpose of computing the collisional energy loss, we can replace $(1 \pm n^{\xi}_{eq}(k'))$ by 1 in Eq. (10), which leads to

$$d^3N_J d\Gamma_{el} \approx \frac{1}{2}\sum_{\text{spins}} |M_{el}|^2 \frac{d^3\vec{\mathbf{p}}'}{(2\pi)^3 2E'} \frac{d^3\vec{\mathbf{k}}}{(2\pi)^3 2k} \frac{d^3\vec{\mathbf{k}}'}{(2\pi)^3 2k'} n_{eq}(k). \tag{12}$$

Here, $n_{eq}(k) = \sum_{\xi=q,\bar{q},g} n^{\xi}_{eq}(k)$ is the equilibrium momentum distribution [24] at temperature T including quark, antiquark and gluon contributions [see Eq. (B2)].

The collisional energy loss can now be obtained from Eqs. (9), (11), and (12), leading to

$$\Delta E_{el} \approx C_R \frac{1}{E^2} \int \frac{d^3\vec{\mathbf{k}}}{(2\pi)^3 2k} n_{eq}(k) \int \frac{d^3\vec{\mathbf{k}}'}{(2\pi)^3 2k'}\, \omega \times \frac{\sin\left[(\omega - \vec{\mathbf{v}}\cdot\vec{\mathbf{q}})\frac{L}{2v}\right]^2}{(\omega - \vec{\mathbf{v}}\cdot\vec{\mathbf{q}})^2} \frac{1}{2}\sum_{\text{spins}} |\mathcal{M}|^2. \tag{13}$$

Note that in Eq. (13) we added a color factor C_R and that $\vec{\mathbf{q}} = \vec{\mathbf{k}}' - \vec{\mathbf{k}}$.

Equation (13) can be further simplified by noting that, in a static medium, the collisional energy loss does not depend on the direction of $\vec{\mathbf{v}}$. After evaluating the $\frac{1}{2}\sum|\mathcal{M}|^2$ and averaging the integrand over the directions of $\vec{\mathbf{v}}$, we obtain (see Appendix B)

$$\Delta E_{el} = \frac{C_R g^4}{2\pi^4} \int_0^\infty n_{eq}(|\vec{\mathbf{k}}|) d|\vec{\mathbf{k}}| \left(\int_0^{|\vec{\mathbf{k}}|} |\vec{\mathbf{q}}| d|\vec{\mathbf{q}}| \int_{-|\vec{\mathbf{q}}|}^{|\vec{\mathbf{q}}|} \omega d\omega + \int_{|\vec{\mathbf{k}}|}^{|\vec{\mathbf{q}}|_{\max}} |\vec{\mathbf{q}}| d|\vec{\mathbf{q}}| \int_{|\vec{\mathbf{q}}|-2|\vec{\mathbf{k}}|}^{|\vec{\mathbf{q}}|} \omega d\omega \right) \left(|\Delta_L(q)|^2 \frac{(2|\vec{\mathbf{k}}|+\omega)^2 - |\vec{\mathbf{q}}|^2}{2} \mathcal{J}_1 + |\Delta_T(q)|^2 \times \frac{(|\vec{\mathbf{q}}|^2 - \omega^2)((2|\vec{\mathbf{k}}|+\omega)^2 + |\vec{\mathbf{q}}|^2)}{4|\vec{\mathbf{q}}|^4} \times \left[(v^2|\vec{\mathbf{q}}|^2 - \omega^2)\mathcal{J}_1 + 2\omega\mathcal{J}_2 - \mathcal{J}_3\right] \right), \tag{14}$$

where $\mathcal{J}_1, \mathcal{J}_2$ and $\mathcal{J}_3$ are given by Eqs. (B6)–(B8) in Appendix B, and $|\vec{\mathbf{q}}|_{\max}$ is given by the following formula [14]:

$$|\vec{\mathbf{q}}|_{\max} = \text{Min}\left[E, \frac{2|\vec{\mathbf{k}}|(1 - |\vec{\mathbf{k}}|/E)}{1 - v + 2|\vec{\mathbf{k}}|/E}\right]. \tag{15}$$

Further numerical study of the collisional energy loss in a finite size QCD medium is given in Sec. IV.

III. COLLISIONAL ENERGY LOSS IN INFINITE QCD MEDIUM

Previous calculations of the collisional energy loss, in particular in Refs. [11,14,15] were done for an infinite QCD medium. A problem with these calculations was that they produce unphysical energy gain in the lower momentum regions. Additionally, these computations leaded to different results and consequently provided quite a large uncertainty in the heavy quark (especially bottom) collisional energy loss.

In this section and Appendix B1 we present an improved calculation of collisional energy loss in an infinite QCD medium, with the goal of 1) removing the problems associated with previous calculations and 2) producing reliable infinite medium results which we will in Sec. IV compare with the collisional energy loss in a finite medium.

In the case of an infinite QCD medium, the collisional energy loss per unit length $\frac{dE_{el}}{dL}$ is computed by assuming that the jet is produced at $x_0 = -\infty$. The energy loss for a finite size medium is than (simplistically) calculated by multiplying this $\frac{dE_{el}}{dL}$ with the thickness L of the medium.

In Appendix B1 we present an improved calculation of the collisional energy loss per unit length in an infinite QCD medium. The following result is obtained:

$$\frac{dE_{el}}{dL} = \frac{g^4}{6v^2\pi^3} \int_0^\infty n_{eq}(|\vec{\mathbf{k}}|) d|\vec{\mathbf{k}}| \left(\int_0^{2|\vec{\mathbf{k}}|/(1+v)} d|\vec{\mathbf{q}}| \times \int_{-v|\vec{\mathbf{q}}|}^{v|\vec{\mathbf{q}}|} \omega d\omega + \int_{2|\vec{\mathbf{k}}|/(1+v)}^{|\vec{\mathbf{q}}|_{\max}} d|\vec{\mathbf{q}}| \int_{|\vec{\mathbf{q}}|-2|\vec{\mathbf{k}}|}^{v|\vec{\mathbf{q}}|} \omega d\omega \right) \times \left(|\Delta_L(q)|^2 \frac{(2|\vec{\mathbf{k}}|+\omega)^2 - |\vec{\mathbf{q}}|^2}{2} + |\Delta_T(q)|^2 \times \frac{(|\vec{\mathbf{q}}|^2 - \omega^2)((2|\vec{\mathbf{k}}|+\omega)^2 + |\vec{\mathbf{q}}|^2)}{4|\vec{\mathbf{q}}|^4} (v^2|\vec{\mathbf{q}}|^2 - \omega^2) \right). \tag{16}$$

To compare our result with the computations done in Refs. [14,15], we here introduce an arbitrary intermediate momentum scale $|\vec{\mathbf{q}}|^*$ [15]. The contribution from $|\vec{\mathbf{q}}| < |\vec{\mathbf{q}}|^*$ is denoted *soft*, while contribution from $|\vec{\mathbf{q}}| > |\vec{\mathbf{q}}|^*$ is denoted *hard* [15].

The soft contribution is given by

$$\frac{dE^{\text{soft}}_{el}}{dL} = \frac{g^4}{6v^2\pi^3} \int_0^\infty n_{eq}(|\vec{\mathbf{k}}|) d|\vec{\mathbf{k}}| \int_0^{|\vec{\mathbf{q}}|^*} d|\vec{\mathbf{q}}| \int_{-v|\vec{\mathbf{q}}|}^{v|\vec{\mathbf{q}}|} \omega d\omega \left(|\Delta_L(q)|^2 \frac{(2|\vec{\mathbf{k}}|+\omega)^2 - |\vec{\mathbf{q}}|^2}{2} + |\Delta_T(q)|^2 \times \frac{(|\vec{\mathbf{q}}|^2 - \omega^2)((2|\vec{\mathbf{k}}|+\omega)^2 + |\vec{\mathbf{q}}|^2)}{4|\vec{\mathbf{q}}|^4} (v^2|\vec{\mathbf{q}}|^2 - \omega^2) \right) \tag{17}$$

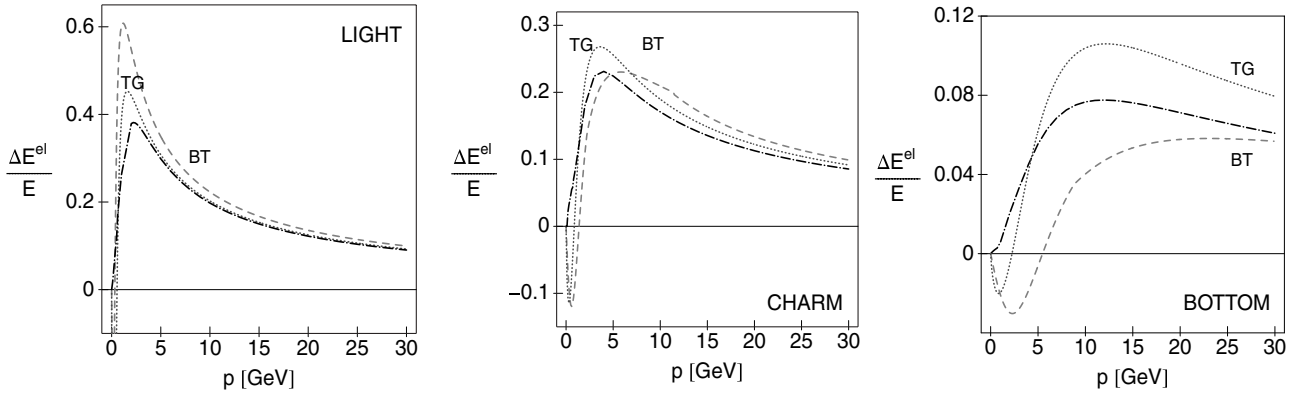

FIG. 2. Fractional collisional energy loss is shown as a function of momentum for light, charm and bottom quark jets (left, center and right panels respectively). Dash-dotted curves are obtained by using Eq. (16) from this paper. Dashed curves correspond to Eqs. (8) and (12) from Ref. [15], while dotted curves are obtained by using Eq. (4.1) from Ref. [14]. Assumed thickness of the medium is $L = 5$ fm.

while the hard contribution is given by

$$\frac{dE_{el}^{\rm hard}}{dL} = \frac{g^4}{6v^2\pi^3}\int_0^\infty n_{eq}(|\vec{\mathbf{k}}|)d|\vec{\mathbf{k}}|\left(\int_{|\vec{\mathbf{q}}|^*}^{2|\vec{\mathbf{k}}|/(1+v)} d|\vec{\mathbf{q}}| \times \int_{-v|\vec{\mathbf{q}}|}^{v|\vec{\mathbf{q}}|}\omega d\omega + \int_{2|\vec{\mathbf{k}}|/(1+v)}^{|\vec{\mathbf{q}}|_{\max}} d|\vec{\mathbf{q}}|\int_{|\vec{\mathbf{q}}|-2|\vec{\mathbf{k}}|}^{v|\vec{\mathbf{q}}|}\omega d\omega\right)\left(|\Delta_L(q)|^2\frac{(2|\vec{\mathbf{k}}|+\omega)^2-|\vec{\mathbf{q}}|^2}{2}+|\Delta_T(q)|^2 \times \frac{(|\vec{\mathbf{q}}|^2-\omega^2)((2|\vec{\mathbf{k}}|+\omega)^2+|\vec{\mathbf{q}}|^2)}{4|\vec{\mathbf{q}}|^4}(v^2|\vec{\mathbf{q}}|^2-\omega^2)\right) \tag{18}$$

The soft contribution can be further simplified by keeping only the even contributions in the ω integral (the odd contributions vanish under symmetric integration)

$$\frac{dE_{el}^{\rm soft}}{dL} = \frac{g^4}{3v^2\pi^3}\int_0^\infty |\vec{\mathbf{k}}|n_{eq}(|\vec{\mathbf{k}}|)d|\vec{\mathbf{k}}|\int_0^{|\vec{\mathbf{q}}|^*} d|\vec{\mathbf{q}}|\int_{-v|\vec{\mathbf{q}}|}^{v|\vec{\mathbf{q}}|}\omega^2 d\omega \times\left(|\Delta_L(q)|^2+\frac{1}{2}\left(1-\frac{\omega^2}{|\vec{\mathbf{q}}|^2}\right)\left(v^2-\frac{\omega^2}{|\vec{\mathbf{q}}|^2}\right)\times|\Delta_T(q)|^2\right)$$
$$= \frac{g^2}{6\pi v^2}\mu_D^2\int_0^{|\vec{\mathbf{q}}|^*} d|\vec{\mathbf{q}}|\int_{-v|\vec{\mathbf{q}}|}^{v|\vec{\mathbf{q}}|}\omega^2 d\omega \times\left(|\Delta_L(q)|^2+\frac{1}{2}\left(1-\frac{\omega^2}{|\vec{\mathbf{q}}|^2}\right)\left(v^2-\frac{\omega^2}{|\vec{\mathbf{q}}|^2}\right)\times|\Delta_T(q)|^2\right), \tag{19}$$

where in the last step we used the fact that

$$\int_0^\infty |\vec{\mathbf{k}}|n_{eq}(|\vec{\mathbf{k}}|)d|\vec{\mathbf{k}}| = \frac{\pi^2T^2}{2}\left(1+\frac{N_f}{6}\right). \tag{20}$$

Equation (19) agrees with the Eq. (55) in Ref. [24].

For the hard contribution we use that, in the limit of large momentum transfer ($|\vec{\mathbf{q}}| \gg |\vec{\mathbf{q}}|^*$), $|\Delta_L(q)| \to \frac{1}{|\vec{\mathbf{q}}|^2}$ and $|\Delta_T(q)| \to \frac{1}{\omega^2-|\vec{\mathbf{q}}|^2}$. It is than straightforward to show that the hard contribution reduces to Eq. (17) in Ref. [24], i.e.,

$$\frac{dE_{el}^{\rm hard}}{dL} = \frac{g^4}{6v^2\pi^3}\int_0^\infty n_{eq}(|\vec{\mathbf{k}}|)d|\vec{\mathbf{k}}|\left(\int_{|\vec{\mathbf{q}}|^*}^{2|\vec{\mathbf{k}}|/(1+v)}\frac{d|\vec{\mathbf{q}}|}{|\vec{\mathbf{q}}|^2} \times\int_{-v|\vec{\mathbf{q}}|}^{v|\vec{\mathbf{q}}|}\omega d\omega + \int_{2|\vec{\mathbf{k}}|/(1+v)}^{|\vec{\mathbf{q}}|_{\max}}\frac{d|\vec{\mathbf{q}}|}{|\vec{\mathbf{q}}|^2}\int_{|\vec{\mathbf{q}}|-2|\vec{\mathbf{k}}|}^{v|\vec{\mathbf{q}}|}\omega d\omega\right) \times\left(\frac{3\omega^2}{4|\vec{\mathbf{q}}|^2}-\frac{v^2}{4}-\frac{1-v^2}{2}\frac{|\vec{\mathbf{q}}|^2}{|\vec{\mathbf{q}}|^2-\omega^2} +3\frac{|\vec{\mathbf{k}}|(|\vec{\mathbf{k}}|+\omega)}{|\vec{\mathbf{q}}|^2}-(1-v^2)\frac{|\vec{\mathbf{k}}|(|\vec{\mathbf{k}}|+\omega)}{|\vec{\mathbf{q}}|^2-\omega^2}\right). \tag{21}$$

Equations (17) and (55) from Ref. [24] were used in Ref. [15] to obtain their Eqs. (8) and (12). That is, while our Eq. (16) is more general, in special cases [i.e., Eqs. (19) and (21)] it reproduces results from Ref. [15].

The computation in Ref. [14] considered only the soft gluon limit, and replaced $|\vec{\mathbf{q}}|^*$ by $|\vec{\mathbf{q}}|_{\max}$, where $|\vec{\mathbf{q}}|_{\max}$ is given by Eq. (15). Consequently, for the purpose of comparison with Ref. [14], we replaced $|\vec{\mathbf{q}}|^*$ by $|\vec{\mathbf{q}}|_{\max}$ in Eq. (19). Additionally, the problem with this approach is that, in the high momentum $|\vec{\mathbf{q}}|$ region, the method [14] is not able to treat the lower ω bound properly (compare Eq. (19) with Eq. (16) where ω bounds are properly treated). To overcome this problem, the calculation in Ref. [14] was limited to the forward emission only (i.e., $\omega > 0$). If this is also taken into account, our Eq. (19) reproduces Eq. (4.1) in Ref. [14].

In summary, in the known limiting cases, our result [i.e., Eq. (16)] reduces to the results published in Refs. [14,15]. The advantage of our result over [14] is that it includes the hard contribution and consistently treats the integration limits. Compared to Ref. [15], the advantage of our result is that it does not make a sharp transition from soft to hard limits, and consequently it does not require the introduction of an unphysical momentum scale $|\vec{\mathbf{q}}|^*$ as in Ref. [15].

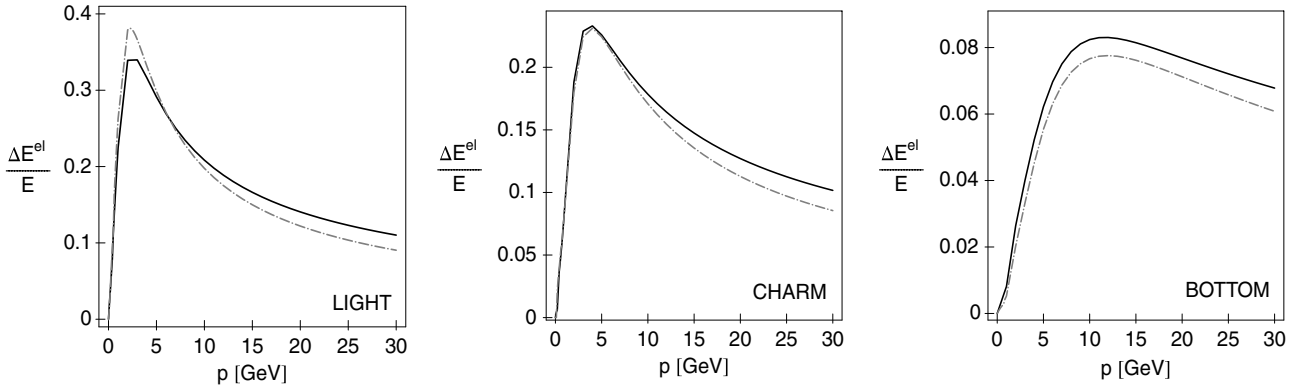

FIG. 3. Fractional collisional energy loss is shown as a function of momentum for light, charm and bottom quark jets (left, center and right panels, respectively). Full curves correspond to finite medium case [see Eq. (14)], while dash-dotted curves correspond to infinite medium case [see Eq. (16)]. Assumed thickness of the medium is $L = 5$ fm.

IV. NUMERICAL RESULTS

In this section we give a numerical study of the collisional energy loss in a QCD medium as presented in Secs. III and IV. To do this, we further assume that the QCD plasma is characterized by $T = 0.225$ GeV, $N_f = 2.5$ and $\alpha = 0.3$ (see Ref. [33], and references therein). For the light quark mass we take $M = \mu_D/\sqrt{6}$, where $\mu_D = gT\sqrt{(1 + \frac{N_f}{6})} \approx 0.5\,\text{GeV}$ is the Debye mass. The charm mass is taken to be $M = 1.2$ GeV, and the bottom mass is $M = 4.75$ GeV.

A. Collisional energy loss in infinite QCD medium

In Fig. 2 we compare our collisional energy loss results in an infinite QCD medium [Eq. (16)] with previous computations by Refs. [14,15]. We see that, while both BT [15] and TG [14] computations lead to unphysical negative energy loss results in the low momentum region, our computations give positive collisional energy loss in the whole jet momentum range. This is particularly important in the bottom quark case where the unphysical behavior persists up to 5 GeV in BT [15] case and up to 2 GeV in TG [14] case. The reason for this behavior is that only the leading logarithmic contribution was considered in the final steps of both BT and TG computations. Note that the problem of unphysical energy gain was addressed in Ref. [34], by including fully dressed gluon propagator in their calculations. However, that approach leaded to another problem, since the unphysical momentum scale $|\vec{\mathbf{q}}|^*$ appeared in the collisional energy loss results [34]. Therefore, our results present a first complete solution to the unphysical energy gain problem.

Our numerical results agree with BT only in the asymptotic regions, which is likely the consequence of the following: 1) BT made a sharp (instead of continuous) transition from soft to hard limit and 2) they introduced a sharp boundary in the energy loss computations depending on whether the initial jet energy is much larger/smaller than M^2/T.

Despite the fact that the BT computations are more up to date and treat the collisional energy loss more consistently than TG, we see that our results show better agreement with TG [14] computations. Particularly, in case of light and charm quark jets, there is a quite good agreement between our results and those of TG [14]. The good agreement is probably because the forward emission only (see Sec. III) provides a quite plausible estimate for the collisional energy loss. However, for bottom quarks we see that neither BT nor TG computations provide a reasonable estimate for the collisional energy loss. Therefore, in this case, the more accurate computation of collisional energy loss [i.e., our Eq. (16)] is needed.

B. Collisional energy loss in a finite QCD medium

Figures 3 and 4 show the comparison between collisional energy loss in infinite and finite size QCD medium. Contrary to Ref. [20], we find that a finite size medium does not have a large effect on the collisional energy loss. The discrepancy between our results and those presented in Ref. [20] is due to the fact that what was called collisional energy loss in Ref. [20], is in fact combination of collisional and part of the zeroth order radiative energy loss. Actually, the calculation in Ref. [20] does not present a complete zeroth order energy loss either, since transition radiation [23] was not included in their computation.

Contrary to naive expectations, from Figs. 3 and 4 we found that collisional energy loss in a finite size medium can be

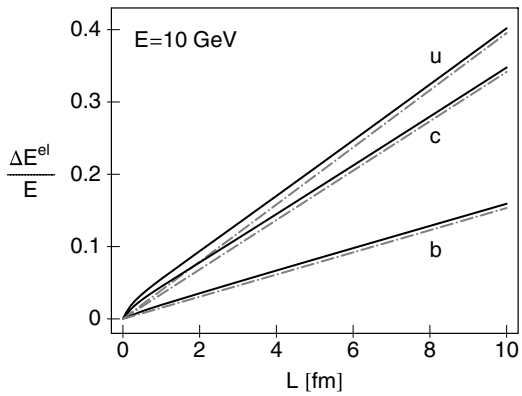

FIG. 4. Fractional collisional energy loss is shown as a function of thickness of the medium for light, charm and bottom quark jets (upper, middle and lower set of curves, respectively). Full curves correspond to finite medium case [see Eq. (14)], while dash-dotted curves correspond to infinite medium case [see Eq. (16)]. Initial momentum of the jet is 10 GeV.

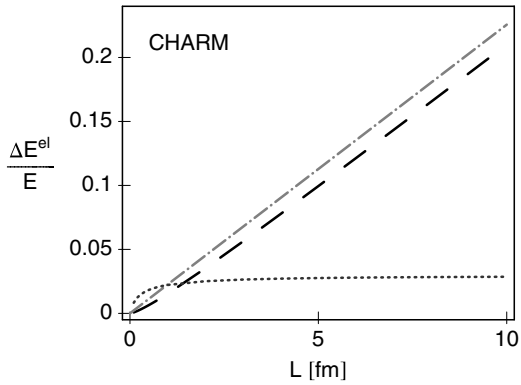

FIG. 5. Fractional collisional energy loss is shown as a function of thickness of the medium for charm quark jet. Dash-dotted curves correspond to infinite medium case [see Eq. (16)], while dashed curve show what would be the collisional energy loss in finite size medium if term $2\omega\mathcal{J}_2 - \mathcal{J}_3 = 0$. Dotted curve shows the extra contribution to the collisional energy loss in finite size medium, due the fact that $2\omega\mathcal{J}_2 - \mathcal{J}_3 \neq 0$. Initial momentum of the jet is 20 GeV.

somewhat larger than in an infinite medium. The reason is that in Eq. (16) there exists a term $2\omega\mathcal{J}_2 - \mathcal{J}_3$. If this term were equal to zero (as in the case of infinite medium), the energy loss in a finite medium case would always be smaller than in an infinite medium, as naively expected (compare dashed and dot-dashed curves in Fig. 5). However, in the finite medium case, the term $2\omega\mathcal{J}_2 - \mathcal{J}_3 \neq 0$, giving a noticeable positive contribution (see the dotted curve in Fig. 5) which will lead to somewhat larger (overall) energy loss in the finite medium case.

To further discuss this, let us look at the Eqs. (B6)–(B8) (Appendix A) in the finite medium case, and compare them to the corresponding Eqs. (B24)–(B26) in the infinite medium. The δ function in Eqs. (B24)–(B26) ensures energy conservation, which is satisfied when the jet is produced at $-\infty$. Consequently, in this case $2\omega\mathcal{J}_2 - \mathcal{J}_3 \equiv 0$ [see Eqs. (B25) and (B26)]. However, when the jet is produced at finite time x_0, time translation invariance is broken, and therefore the energy of the collisional process is not conserved, leading to $2\omega\mathcal{J}_2 - \mathcal{J}_3 \neq 0$.

C. Comparison between collisional and radiative energy loss in a finite size QCD medium

In Appendix A we showed how to separate the contributions to the collisional and radiative energy loss. In this section we directly compare these two contributions in the case of finite size QCD medium.

To compute the net radiative energy loss, we note that there are three important effects that control this energy loss in a QCD medium. These effects are the Ter-Mikayelian effect [21], transition radiation [23] and medium induced radiation [35]. In Ref. [23], we combined these effects to compute the net radiative energy loss. We here use these results for the purpose of further comparison with the collisional energy loss. Note that in these computations, in order to simulate confinement in the vacuum, we introduced an effective gluon mass in the vacuum $m_{g,v} \approx \Lambda_{\rm QCD} = 0.2$ GeV (for more details see Ref. [23]).

In Figs. 6 and 7 we show the collisional and radiative energy loss as a function of jet energy and thickness of the medium, respectively. We see that collisional energy loss is comparable with the net radiative energy loss in the medium. Therefore, the collisional energy loss contribution is significant and must be included in the computation of jet quenching in a QCD medium.

In particular, we note that in the lower momentum (i.e., $p < 10$ GeV) range, the collisional energy loss dominates the radiative one. At RHIC, jet suppression is mostly measured in this (lower) momentum range. Therefore, contrary to previous studies [4–7], our results indicate that it is collisional, instead of radiative energy loss, which gives the dominant contribution to the observed suppression values.

Finally, note that the numerical computations/comparisons, for both collisional and radiative energy loss, were here obtained by using the fixed coupling constant $\alpha_S = 0.3$. However, the collisional and radiative energy losses depend on the coupling, $\Delta E^{el} \sim \alpha_S^2$, and $\Delta E^{\rm rad} \sim \alpha_S^3$ [35]. For example, in a subsequent paper [36], it was obtained that the running of the coupling increase the magnitude of the collisional energy loss. Therefore, using more accurate expressions for coupling constant may change the numerical results presented in this

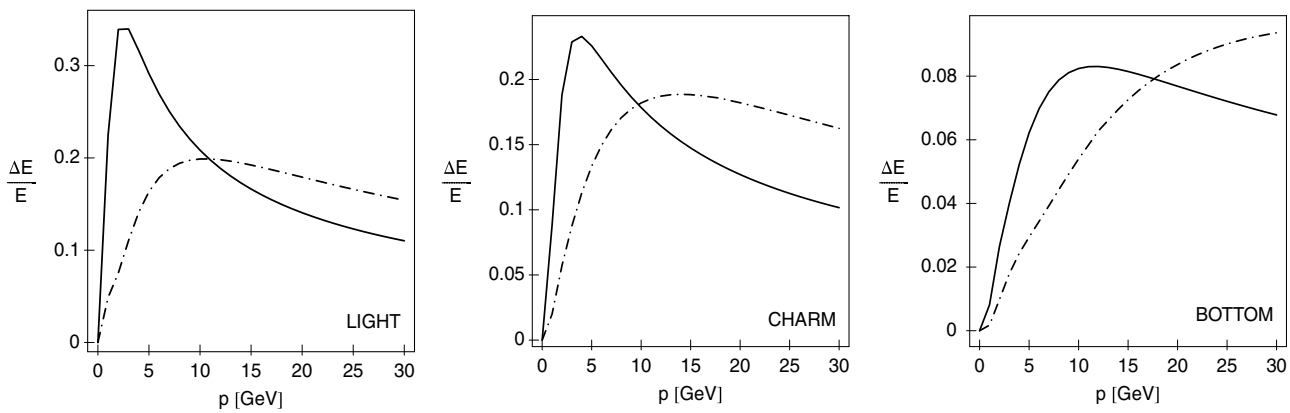

FIG. 6. The comparison between collisional and radiative fractional energy loss is shown as a function of momentum for light, charm and bottom quark jets (left, center, and right panels, respectively). Full curves show the collisional energy loss, while dot-dashed curves show the net radiative energy loss. Assumed thickness of the medium is $L = 5$ fm and $\lambda = 1.2$ fm [19].

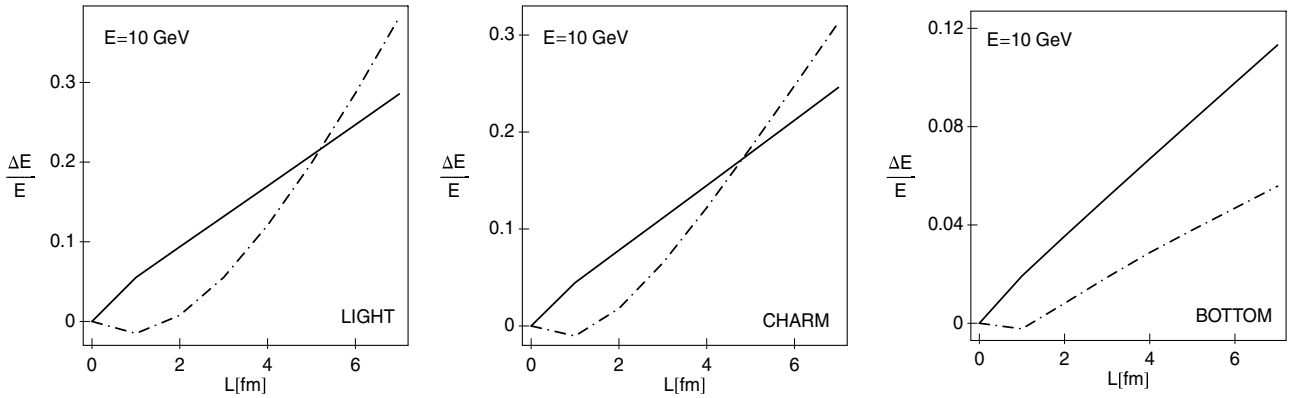

FIG. 7. The comparison between collisional and radiative fractional energy loss is shown as a function of the thickness of the medium. Light, charm, and bottom quark cases are shown on the left, center and right panels, respectively. Full curves show the collisional energy loss, while dot-dashed curves show the net radiative energy loss. Mean free path is $\lambda = 1.2$ fm [19]. Initial momentum of the jet is $E = 10$ GeV.

paper (note that the derived Eq. (14) is valid for wide range of coupling constants). However, according to Ref. [36], the main result of this paper, i.e., the importance of the collisional energy loss, is expected to be even more emphasized when more accurate expressions of coupling constants are used.

V. CONCLUSION

This paper addressed the zeroth order contribution to the collisional energy loss in a finite size QCD medium. The interest in the collisional energy loss has been renewed by recent studies [11,12], particularly in the context of the single electron puzzle [8–10]. In Refs. [11,12] it was claimed that, contrary to the previous beliefs, for the parameter ranges relevant in URHIC, radiative and collisional energy loss become comparable. However, a recent study by Peigne *et al*. [20] suggested that collisional energy loss is large in the ideal infinite medium case, while the finite size medium effects lead to significant reduction of the collisional energy loss. The paper [20], however, did not completely separate collisional from radiative energy loss.

Additionally, even in the infinite medium case, the problem of collisional energy loss was not completely solved. Previous computations obtained unphysical results in the low momentum regions [14,15], and an approach to solve this problem [34] leaded to the results dependent on the unphysical momentum scales. In addition, these computations introduced quite a large uncertainty in the heavy quark (especially bottom) collisional energy loss, since they leaded to noticeably different numerical results.

The above reasons and the previously discussed single electron puzzle, motivated us to provide a detailed study of the zeroth order collisional energy loss in a finite size QCD medium created in URHIC. First, in Appendix A we showed that, though zeroth order collisional and radiative energy loss contributions come from the same one-loop HTL diagram, there is no overlap between collisional and radiative energy loss computations. More specifically, while zeroth order collisional energy loss comes from the processes which have the same number of incoming and outgoing particles, the radiative energy loss has one gluon more as an outcome of the process. Additionally, we showed that in the zeroth order calculations, there are no interference effects between collisional and radiative energy loss, which is different from a result in the recent paper [37]. The absence of interference effects comes from the fact that, contrary to Ref. [37], in our study we consistently treat the gluon dispersion relation in the medium. This leads to the following conditions: 1) for the 0^{th} order collisional energy loss contributions, the energy of the exchanged (virtual) gluon has to be smaller, or equal, to the gluon momentum, and 2) for the radiative energy loss contributions the energy of the radiated gluon has to be larger than its momentum. Therefore, these two contributions take nonzero values in non-overlapping regions, and consequently cannot interfere with each other. A subsequent paper by Adil *et al*. [38] reached similar conclusions to those presented here, by using a different approach (linear response theory).

In the case of infinite medium, our computation interpolates smoothly between soft to hard contributions and, contrary to Ref. [15], does not require the introduction of an arbitrary intermediate momentum scale. Additionally, our computation treats the lower momentum region consistently, removing the unphysical energy gain results obtained in previous computations [14,15].

In the case of finite size QCD medium, contrary to the study by Peigne *et al*. [20] we showed that finite size effects have small effect on the collisional energy loss. Therefore, consistently with the claims in Refs. [11,12] and our recent single electron suppression estimates [19], we here showed that collisional energy loss is important, and has to be included in the computation of jet quenching.

ACKNOWLEDGMENTS

I thank Ulrich Heinz for discussions and critical reading of the manuscript. Valuable discussions with Eric Braaten, Miklos Gyulassy, Yuri Kovchegov, and Xin-Nian Wang are gratefully acknowledged. This work is supported by the U.S. Department of Energy, grant DE-FG02-01ER41190.

APPENDIX A: HTL CONTRIBUTION TO THE COLLISIONAL ENERGY LOSS

In this section we will derive the formula for the lowest order collisional interaction rate. The zeroth order contribution to both radiative and collisional rates comes from the diagram M given in Fig. 8. We will below use this diagram as a starting point to separate contributions of collisional and radiative energy loss.

Diagram M corresponds to $\sum M_n$, where M_n is the amplitude of the diagram shown in Fig. 9.

The definition of "black circles" in Fig. 9 is shown in Fig. 10.

The diagram M contains both collisional and radiative zeroth order contribution to the jet energy loss. It is useful to look at the simple $n = 1$ case (see Fig. 11) to better understand this.

The contribution to the collisional energy loss is obtained by "cutting" (i.e., putting on shell) the propagators of parton k' and p'. On the other hand, the radiative contribution is obtained by putting the parton propagator p' and the gluon propagator q on shell. From this, it follows that collisional and radiative contributions come from different diagrams. Furthermore, from the conservation of energy and momentum it can be shown that cutting the gluon propagator q, leads to the condition $|\omega| > |\vec{\mathbf{q}}|$, while cutting the propagator of parton k' leads to the condition $|\omega| < |\vec{\mathbf{q}}|$. Consequently, there is no interference (and overcounting) between collisional and radiative contributions.[2] The computation of the radiative zeroth order energy loss has already been a subject of our previous work [21,23]. So, the contributions from the diagrams which give raise to the radiative energy loss, will not be further addressed here.

As we can see from the right side of Fig. 11, there are two contributions from diagram M_1 to the collisional rate. These two contributions can be combined into one by allowing that the energy of the gluon can take both positive and negative values. Therefore, the contribution to the collisional rate from diagram M_1 ($d\Gamma_{M_1}$) is equal to

$$d^3N_J\, d\Gamma_{M_1} = \frac{d^3\vec{\mathbf{p}}'}{(2\pi)^3 2E'}\frac{d^3\vec{\mathbf{k}}}{(2\pi)^3 2k} \times \frac{d^3\vec{\mathbf{k}}'}{(2\pi)^3 2k'}\, n_{eq}(k)\, |M_{E_0}|^2, \qquad \text{(A1)}$$

[2]Note that in this paper, we treat only the zeroth order contribution to collisional energy loss. It is, however, possible that interference effects and/or overcounting between collisional and radiative energy loss contributions would occur in the higher order computations. Higher order contributions are a separate non-trivial problem, which is not considered in this paper.

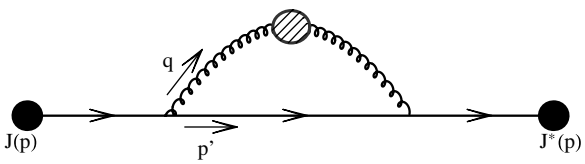

FIG. 8. One Hard Thermal Loop (HTL) diagram.

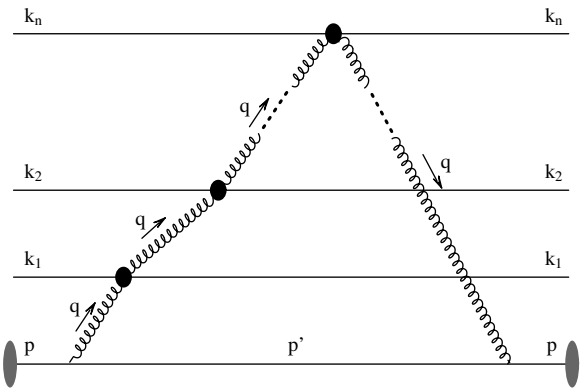

FIG. 9. Diagram M_n.

where M_{E_0} is the Feynman diagram shown in Fig. 12, and $\omega \in (-|\vec{\mathbf{q}}|, |\vec{\mathbf{q}}|)$. Note that in the above equation each of the terms in $n_{eq}(k) = \sum_{\xi=q,\bar{q},g} n^{\xi}_{eq}(k)$ should be multiplied by an extra factor $[1 \pm n^{\xi}_{eq}(k')]$ for the outgoing medium parton (see Sec. II). Here ξ corresponds to anti(quark) or gluon. The $+$ sign is associated with gluon and the $-$ sign with anti(quark) contributions. However, the $\pm n^{\xi}_{eq}(k')$ term in $(1 \pm n^{\xi}_{eq}(k'))$ does not contribute to the collisional energy loss (for more details see Sec. II and Ref. [24]). Therefore, in Eq. (A1) we keep only the contributions that give raise to the collisional energy loss.

In the same way, it can be shown that the contribution to the collisional energy loss from diagram M_n is equal to

$$d^3N_J\, d\Gamma_{M_n} = \frac{d^3\vec{\mathbf{p}}'}{(2\pi)^3 2E'}\frac{d^3\vec{\mathbf{k}}}{(2\pi)^3 2k}\frac{d^3\vec{\mathbf{k}}'}{(2\pi)^3 2k'}\, n_{eq}(k) \times \sum_{i=0}^{n-1} M_{E_i} M^{\dagger}_{E_{n-1-i}}, \qquad \text{(A2)}$$

where the diagram M_{E_n} is shown in Fig. 13.

Since $M = \sum_{n=0}^{\infty} M_n$, the contribution to the collisional energy loss from the diagram M is equal to

$$\begin{aligned} d^3N_J\, d\Gamma &= \frac{d^3\vec{\mathbf{p}}'}{(2\pi)^3 2E'}\frac{d^3\vec{\mathbf{k}}}{(2\pi)^3 2k}\frac{d^3\vec{\mathbf{k}}'}{(2\pi)^3 2k'}\, n_{eq}(k) \times \sum_{n=0}^{\infty}\sum_{i=0}^{n-1} M_{E_i} M^{\dagger}_{E_{n-1-i}} \\ &= \frac{d^3\vec{\mathbf{p}}'}{(2\pi)^3 2E'}\frac{d^3\vec{\mathbf{k}}}{(2\pi)^3 2k}\frac{d^3\vec{\mathbf{k}}'}{(2\pi)^3 2k'}\, n_{eq}(k) \times \sum_{n=0}^{\infty}\sum_{i=0}^{n} M_{E_i} M^{\dagger}_{E_{n-i}}. \end{aligned} \qquad \text{(A3)}$$

We next want to prove that $d^3N_J\, d\Gamma = \frac{d^3\vec{\mathbf{p}}'}{(2\pi)^3 2E'} \frac{d^3\vec{\mathbf{k}}}{(2\pi)^3 2k}\frac{d^3\vec{\mathbf{k}}'}{(2\pi)^3 2k'}\, n_{eq}(k)\, |M_{el}|^2$, where (see Fig. 14)

$$M_{el} = \sum_{n=0}^{\infty} M_{E_n}. \qquad \text{(A4)}$$

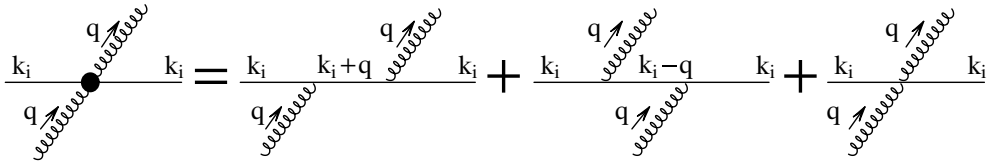

FIG. 10. Definition of the "black circles" in diagram M_n.

To prove the above, we will first compute $|M_{el}|^2$

$$|M_{el}|^2 = \sum_{i=0}^{\infty}\sum_{j=0}^{\infty} M_{E_i} M^{\dagger}_{E_j} = \sum_{i=0}^{\infty}\sum_{n=i}^{\infty} M_{E_i} M^{\dagger}_{E_{n-i}}, \quad \text{(A5)}$$

where in the last step we defined $n = i + j \to j = n - i$.

Since

$$\sum_{i=0}^{\infty}\sum_{n=i}^{\infty} = \sum_{n=0}^{\infty}\sum_{i=0}^{n}, \quad \text{(A6)}$$

we can conclude that

$$d^3N_J\, d\Gamma = \frac{d^3\vec{\mathbf{p}}'}{(2\pi)^3 2E'} \frac{d^3\vec{\mathbf{k}}}{(2\pi)^3 2k} \frac{d^3\vec{\mathbf{k}}'}{(2\pi)^3 2k'}\, n_{eq}(k) \sum_{n=0}^{\infty} |M_{el}|^2, \quad \text{(A7)}$$

which is what we wanted to prove. Therefore, the collisional interaction rate can be obtained by an intuitive approach of computing $|M_{el}|^2$ (see Fig. 14), where blob represents the effective gluon propagator.

APPENDIX B: COLLISIONAL ENERGY LOSS COMPUTATIONS

In this appendix we will derive the collisional energy formula given by Eq. (14). To do that we start from the Eq. (13), i.e.,

$$\Delta E_{el} = C_R \frac{1}{E^2} \int \frac{d^3\vec{\mathbf{k}}}{(2\pi)^3 2k} n_{eq}(k) \int \frac{d^3\vec{\mathbf{k}}'}{(2\pi)^3 2k'}\, \omega \times \frac{\sin\left[(\omega - \vec{\mathbf{v}}\cdot\vec{\mathbf{q}})\frac{L}{2v}\right]^2}{(\omega - \vec{\mathbf{v}}\cdot\vec{\mathbf{q}})^2} \frac{1}{2}\sum_{\text{spins}} |\mathcal{M}|^2, \quad \text{(B1)}$$

where $n_{eq}(k)$ is the equilibrium momentum distribution [24] at temperature T including quarks and gluons

$$n_{eq}(k) = \frac{N}{e^{|\vec{\mathbf{k}}|/T} - 1} + \frac{N_f}{e^{|\vec{\mathbf{k}}|/T} + 1}. \quad \text{(B2)}$$

Here N is the number of colors and N_f is the number of flavors.

The matrix element $\mathcal{M}$ [see Eq. (8)], has been already computed in Ref. [24] (see Eqs. (45–46) in Ref. [24]). However, for completeness and due to a typographical error in [24], we here repeat the main steps in the computation of $\frac{1}{2}\sum_{\text{spins}} |\mathcal{M}|^2$,

$$\mathcal{M} = g^2 D_{\mu\nu}(q)\bar{u}(p', s')\gamma^{\mu}u(p, s)\bar{u}(k', \lambda')\gamma^{\nu}u(k, \lambda). \quad \text{(B3)}$$

In Coulomb gauge, the only nonzero terms in the effective gluon propagator are given in Eqs. (4) and (5), which together with Eqs. (1)–(3) reduce the Eq. (B3) to

$$\mathcal{M} = g^2\Delta_L(q)\bar{u}(p', s')\gamma^0 u(p, s)\bar{u}(k', \lambda')\gamma^0 u(k, \lambda) + g^2\Delta_T(q)(\delta^{ij} - \hat{q}^i\hat{q}^j)\bar{u}(p', s')\gamma^i u(p, s) \times \bar{u}(k', \lambda')\gamma^j u(k, \lambda). \quad \text{(B4)}$$

Here $\hat{q}^i \equiv q^i/|\vec{\mathbf{q}}|$.

The matrix element given in Eq. (B4) has to be squared, averaged over initial spin s of the jet and summed over all other spins. After evaluating the Dirac traces, and applying the assumption that $|\vec{\mathbf{q}}| \ll E$ (highly energetic jet) we obtain similarly to [24]

$$\begin{aligned}\frac{1}{2}\sum_{\text{spins}} |\mathcal{M}|^2 = {} & 16g^4E^2(|\Delta_L(q)|^2(|\vec{\mathbf{k}}||\vec{\mathbf{k}}'| + \vec{\mathbf{k}}\cdot\vec{\mathbf{k}}') \\ & + 2Re(\Delta_L(q)\Delta_T(q)^*)\left[|\vec{\mathbf{k}}|\left(\vec{\mathbf{v}}\cdot\vec{\mathbf{k}}' - \frac{\vec{\mathbf{v}}\cdot\vec{\mathbf{q}}\;\vec{\mathbf{q}}\cdot\vec{\mathbf{k}}'}{|\vec{\mathbf{q}}|^2}\right) + |\vec{\mathbf{k}}'|\left(\vec{\mathbf{v}}\cdot\vec{\mathbf{k}} - \frac{\vec{\mathbf{v}}\cdot\vec{\mathbf{q}}\;\vec{\mathbf{q}}\cdot\vec{\mathbf{k}}}{|\vec{\mathbf{q}}|^2}\right)\right] \\ & + |\Delta_T(q)|^2\left[2\left(\vec{\mathbf{v}}\cdot\vec{\mathbf{k}} - \frac{\vec{\mathbf{v}}\cdot\vec{\mathbf{q}}\;\vec{\mathbf{q}}\cdot\vec{\mathbf{k}}}{|\vec{\mathbf{q}}|^2}\right)\times\left(\vec{\mathbf{v}}\cdot\vec{\mathbf{k}}' - \frac{\vec{\mathbf{v}}\cdot\vec{\mathbf{q}}\;\vec{\mathbf{q}}\cdot\vec{\mathbf{k}}'}{|\vec{\mathbf{q}}|^2}\right) + (|\vec{\mathbf{k}}||\vec{\mathbf{k}}'| - \vec{\mathbf{k}}\cdot\vec{\mathbf{k}}')\times\left(v^2 - \frac{\vec{\mathbf{v}}\cdot\vec{\mathbf{q}}\;\vec{\mathbf{q}}\cdot\vec{\mathbf{v}}}{|\vec{\mathbf{q}}|^2}\right)\right]. \quad \text{(B5)}\end{aligned}$$

In a static medium, the collisional energy loss does not depend on the direction of $\vec{\mathbf{v}}$. Therefore, the Eq. (B1) can be further simplified by averaging the integrand over the

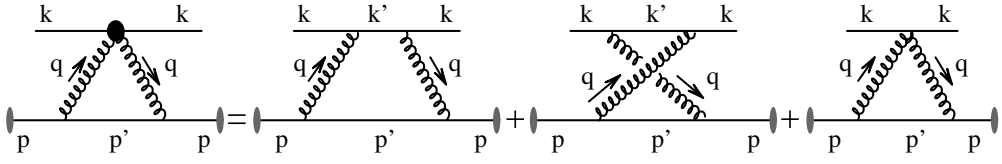

FIG. 11. $n = 1$ contribution to the HTL diagram.

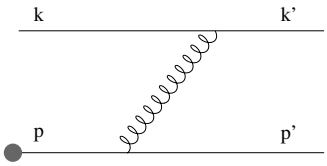

FIG. 12. Feynman diagram for the lowest order collisional energy loss.

directions of $\vec{\mathbf{v}}$. The integrals that are required are

$$\mathcal{J}_1 = \int \frac{d\Omega}{4\pi} \frac{\sin\left[(\omega-\vec{\mathbf{v}}\cdot\vec{\mathbf{q}})\frac{L}{2v}\right]^2}{(\omega-\vec{\mathbf{v}}\cdot\vec{\mathbf{q}})^2} = \frac{L}{4|\vec{\mathbf{q}}|v^2}\left[Si\left((v|\vec{\mathbf{q}}|+\omega)\frac{L}{v}\right)+Si\left((v|\vec{\mathbf{q}}|-\omega)\frac{L}{v}\right)\right] - \frac{1}{4v|\vec{\mathbf{q}}|}\left[\frac{1-\cos\left((v|\vec{\mathbf{q}}|-\omega)\frac{L}{v}\right)}{v|\vec{\mathbf{q}}|-\omega} + \frac{1-\cos\left((v|\vec{\mathbf{q}}|+\omega)\frac{L}{v}\right)}{v|\vec{\mathbf{q}}|+\omega}\right], \tag{B6}$$

$$\mathcal{J}_2 = \int \frac{d\Omega}{4\pi} \frac{\sin\left[(\omega-\vec{\mathbf{v}}\cdot\vec{\mathbf{q}})\frac{L}{2v}\right]^2}{(\omega-\vec{\mathbf{v}}\cdot\vec{\mathbf{q}})^2}(\omega-\vec{\mathbf{v}}\cdot\vec{\mathbf{q}}) = \frac{1}{4v|\vec{\mathbf{q}}|}\left[Ci\left((v|\vec{\mathbf{q}}|-\omega)\frac{L}{v}\right)-Ci\left((v|\vec{\mathbf{q}}|+\omega)\frac{L}{v}\right)+\ln\left(\frac{v|\vec{\mathbf{q}}|+\omega}{v|\vec{\mathbf{q}}|-\omega}\right)\right] \tag{B7}$$

and

$$\mathcal{J}_3 = \int \frac{d\Omega}{4\pi} \frac{\sin\left[(\omega-\vec{\mathbf{v}}\cdot\vec{\mathbf{q}})\frac{L}{2v}\right]^2}{(\omega-\vec{\mathbf{v}}\cdot\vec{\mathbf{q}})^2}(\omega-\vec{\mathbf{v}}\cdot\vec{\mathbf{q}})^2 = \frac{1}{2}\left(1-\frac{\cos\left(\frac{L\omega}{v}\right)\sin(L|\vec{\mathbf{q}}|)}{L|\vec{\mathbf{q}}|}\right). \tag{B8}$$

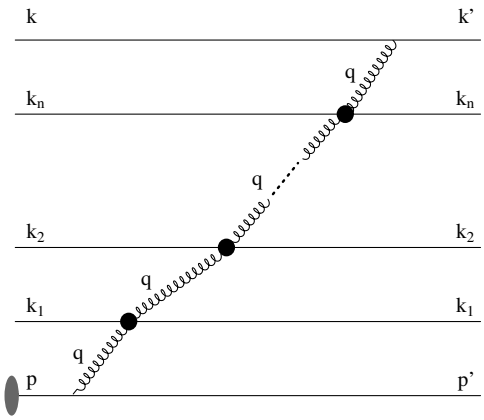

FIG. 13. Feynman diagram for the collisional energy loss with n interactions with medium partons.

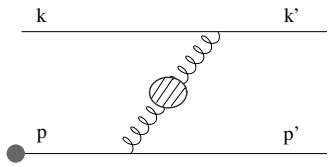

FIG. 14. Feynman diagram M_{el} for the collisional energy loss in QCD medium. The large dashed circle ("blob") represents the effective gluon propagator [21].

By using Eqs. (B6)–(B8), it can be shown that

$$\int \frac{d\Omega}{4\pi} \frac{\sin\left[(\omega-\vec{\mathbf{v}}\cdot\vec{\mathbf{q}})\frac{L}{2v}\right]^2}{(\omega-\vec{\mathbf{v}}\cdot\vec{\mathbf{q}})^2} v^i = \mathcal{J}_1\hat{q}^i\frac{\omega}{|\vec{\mathbf{q}}|} - \mathcal{J}_2\frac{\hat{q}^i}{|\vec{\mathbf{q}}|} \tag{B9}$$

and

$$\int \frac{d\Omega}{4\pi} \frac{\sin\left[(\omega-\vec{\mathbf{v}}\cdot\vec{\mathbf{q}})\frac{L}{2v}\right]^2}{(\omega-\vec{\mathbf{v}}\cdot\vec{\mathbf{q}})^2} v^i v^j = \mathcal{J}_1\left(\frac{v^2|\vec{\mathbf{q}}|^2-\omega^2}{|\vec{\mathbf{q}}|^2}\delta^{ij}+\frac{3\omega^2-v^2|\vec{\mathbf{q}}|^2}{2|\vec{\mathbf{q}}|^2}\hat{q}^i\hat{q}^j\right) + \frac{2\omega\mathcal{J}_2-\mathcal{J}_3}{2|\vec{\mathbf{q}}|^2}\left(\delta^{ij}-3\hat{q}^i\hat{q}^j\right). \tag{B10}$$

By using Eqs. (B5)–(B10) it is straightforward to show that

$$\int \frac{d\Omega}{4\pi} \frac{\sin\left[(\omega-\vec{\mathbf{v}}\cdot\vec{\mathbf{q}})\frac{L}{2v}\right]^2}{(\omega-\vec{\mathbf{v}}\cdot\vec{\mathbf{q}})^2} 16g^4E^2|\Delta_L(q)|^2(|\vec{\mathbf{k}}||\vec{\mathbf{k}}'|+\vec{\mathbf{k}}\cdot\vec{\mathbf{k}}') = 16g^4E^2|\Delta_L(q)|^2\frac{(2|\vec{\mathbf{k}}|+\omega)^2-|\vec{\mathbf{q}}|^2}{2}\mathcal{J}_1, \tag{B11}$$

$$\int \frac{d\Omega}{4\pi} \frac{\sin\left[(\omega-\vec{\mathbf{v}}\cdot\vec{\mathbf{q}})\frac{L}{2v}\right]^2}{(\omega-\vec{\mathbf{v}}\cdot\vec{\mathbf{q}})^2} 32g^4E^2Re(\Delta_L(q)\Delta_T(q)^*) \times\left[|\vec{\mathbf{k}}|\left(\vec{\mathbf{v}}\cdot\vec{\mathbf{k}}'-\frac{\vec{\mathbf{v}}\cdot\vec{\mathbf{q}}\,\vec{\mathbf{q}}\cdot\vec{\mathbf{k}}'}{|\vec{\mathbf{q}}|^2}\right) + |\vec{\mathbf{k}}'|\left(\vec{\mathbf{v}}\cdot\vec{\mathbf{k}}-\frac{\vec{\mathbf{v}}\cdot\vec{\mathbf{q}}\,\vec{\mathbf{q}}\cdot\vec{\mathbf{k}}}{|\vec{\mathbf{q}}|^2}\right)\right] = 0 \tag{B12}$$

and

$$\int \frac{d\Omega}{4\pi} \frac{\sin\left[(\omega-\vec{\mathbf{v}}\cdot\vec{\mathbf{q}})\frac{L}{2v}\right]^2}{(\omega-\vec{\mathbf{v}}\cdot\vec{\mathbf{q}})^2} 16g^4E^2|\Delta_T(q)|^2 \times\left[2\left(\vec{\mathbf{v}}\cdot\vec{\mathbf{k}}-\frac{\vec{\mathbf{v}}\cdot\vec{\mathbf{q}}\,\vec{\mathbf{q}}\cdot\vec{\mathbf{k}}}{|\vec{\mathbf{q}}|^2}\right)\left(\vec{\mathbf{v}}\cdot\vec{\mathbf{k}}'-\frac{\vec{\mathbf{v}}\cdot\vec{\mathbf{q}}\,\vec{\mathbf{q}}\cdot\vec{\mathbf{k}}'}{|\vec{\mathbf{q}}|^2}\right) + (|\vec{\mathbf{k}}||\vec{\mathbf{k}}'|-\vec{\mathbf{k}}\cdot\vec{\mathbf{k}}')\left(v^2-\frac{\vec{\mathbf{v}}\cdot\vec{\mathbf{q}}\,\vec{\mathbf{q}}\cdot\vec{\mathbf{v}}}{|\vec{\mathbf{q}}|^2}\right)\right] = 16g^4E^2|\Delta_T(q)|^2\frac{(|\vec{\mathbf{q}}|^2-\omega^2)((2|\vec{\mathbf{k}}|+\omega)^2+|\vec{\mathbf{q}}|^2)}{4|\vec{\mathbf{q}}|^4} \times\left[(v^2|\vec{\mathbf{q}}|^2-\omega^2)\mathcal{J}_1+2\omega\mathcal{J}_2-\mathcal{J}_3\right]. \tag{B13}$$

Therefore, averaging the $\frac{\sin[(\omega-\vec{\mathbf{v}}\cdot\vec{\mathbf{q}})\frac{L}{2v}]^2}{(\omega-\vec{\mathbf{v}}\cdot\vec{\mathbf{q}})^2}\ \frac{1}{2}\sum|\mathcal{M}|^2$ over the directions of $\vec{\mathbf{v}}$ lead to

$$\left\langle \frac{\sin[(\omega-\vec{\mathbf{v}}\cdot\vec{\mathbf{q}})\frac{L}{2v}]^2}{(\omega-\vec{\mathbf{v}}\cdot\vec{\mathbf{q}})^2}\ \frac{1}{2}\sum_{\text{spins}}|\mathcal{M}|^2\right\rangle$$
$$= 16g^4E^2\left(|\Delta_L(q)|^2\frac{(2|\vec{\mathbf{k}}|+\omega)^2-|\vec{\mathbf{q}}|^2}{2}\mathcal{J}_1 + |\Delta_T(q)|^2\frac{(|\vec{\mathbf{q}}|^2-\omega^2)((2|\vec{\mathbf{k}}|+\omega)^2+|\vec{\mathbf{q}}|^2)}{4|\vec{\mathbf{q}}|^4} \times\left[(v^2|\vec{\mathbf{q}}|^2-\omega^2)\mathcal{J}_1+2\omega\mathcal{J}_2-\mathcal{J}_3\right]\right). \quad \text{(B14)}$$

Since the collisional energy loss does not depend on the direction of $\vec{\mathbf{v}}$, Eq. (B1) can be written as

$$\Delta E_{el} = C_R\frac{1}{E^2}\int\frac{d^3\vec{\mathbf{k}}}{(2\pi)^3 2k}n_{eq}(k)\int\frac{d^3\vec{\mathbf{k}}'}{(2\pi)^3 2k'}\ \omega \times\left\langle\frac{\sin\left[(\omega-\vec{\mathbf{v}}\cdot\vec{\mathbf{q}})\frac{L}{2v}\right]^2}{(\omega-\vec{\mathbf{v}}\cdot\vec{\mathbf{q}})^2}\ \frac{1}{2}\sum_{\text{spins}}|\mathcal{M}|^2\right\rangle$$
$$= \frac{C_R}{32\pi^4}\frac{1}{E^2}\int|\vec{\mathbf{k}}||\vec{\mathbf{k}}'|d|\vec{\mathbf{k}}|d|\vec{\mathbf{k}}'|d\cos\theta n_{eq}(|\vec{\mathbf{k}}|)\omega \times\left\langle\frac{\sin\left[(\omega-\vec{\mathbf{v}}\cdot\vec{\mathbf{q}})\frac{L}{2v}\right]^2}{(\omega-\vec{\mathbf{v}}\cdot\vec{\mathbf{q}})^2}\ \frac{1}{2}\sum_{\text{spins}}|\mathcal{M}|^2\right\rangle, \quad \text{(B15)}$$

where θ is the angle between vectors $\vec{\mathbf{k}}$ and $\vec{\mathbf{k}}'$. Using the fact that $q = k' - k$, we obtain that the $\cos\theta$ satisfies the following relation:

$$\cos\theta = 1-\frac{\vec{\mathbf{q}}^2-\omega^2}{2|\vec{\mathbf{k}}||\vec{\mathbf{k}}'|}, \quad \text{(B16)}$$

where $|\vec{\mathbf{k}}'| = |\vec{\mathbf{k}}|+\omega$. We can now introduce the change of variables from $|\vec{\mathbf{k}}|, |\vec{\mathbf{k}}'|$ and $\cos\theta$, to $|\vec{\mathbf{k}}|, \omega$ and $|\vec{\mathbf{q}}|$, which reduces the Eq. (B1) to the following form:

$$\Delta E_{el} = \frac{C_R}{32\pi^4}\frac{1}{E^2}\int n_{eq}(|\vec{\mathbf{k}}|)d|\vec{\mathbf{k}}|\ |\vec{\mathbf{q}}|d|\vec{\mathbf{q}}|\ \omega d\omega \times\left\langle\frac{\sin\left[(\omega-\vec{\mathbf{v}}\cdot\vec{\mathbf{q}})\frac{L}{2v}\right]^2}{(\omega-\vec{\mathbf{v}}\cdot\vec{\mathbf{q}})^2}\ \frac{1}{2}\sum_{\text{spins}}|\mathcal{M}|^2\right\rangle$$
$$= \frac{C_Rg^4}{2\pi^4}\int n_{eq}(|\vec{\mathbf{k}}|)d|\vec{\mathbf{k}}|\ |\vec{\mathbf{q}}|d|\vec{\mathbf{q}}|\ \omega d\omega \times\left(|\Delta_L(q)|^2\frac{(2|\vec{\mathbf{k}}|+\omega)^2-|\vec{\mathbf{q}}|^2}{2}\mathcal{J}_1 + |\Delta_T(q)|^2\frac{(|\vec{\mathbf{q}}|^2-\omega^2)((2|\vec{\mathbf{k}}|+\omega)^2+|\vec{\mathbf{q}}|^2)}{4|\vec{\mathbf{q}}|^4} \times\left[(v^2|\vec{\mathbf{q}}|^2-\omega^2)\mathcal{J}_1+2\omega\mathcal{J}_2-\mathcal{J}_3\right]\right). \quad \text{(B17)}$$

Limits of the integration can be obtained from Eq. (44), from which it follows that

$$0 < \frac{\vec{\mathbf{q}}^2-\omega^2}{2|\vec{\mathbf{k}}|(|\vec{\mathbf{k}}|+\omega)} < 2, \quad \text{(B18)}$$

leading to the limits in energy transfer ω

$$\text{Max}[-|\vec{\mathbf{q}}|, |\vec{\mathbf{q}}|-2|\vec{\mathbf{k}}|] < \omega < |\vec{\mathbf{q}}|. \quad \text{(B19)}$$

The limits on the momentum transfer $|\vec{\mathbf{q}}|$ from collisional scattering off a thermal parton with energy $|\vec{\mathbf{k}}|$ is (see Ref. [14])

$$0 < |\vec{\mathbf{q}}| < \text{Min}\left[E, \frac{2|\vec{\mathbf{k}}|(1-|\vec{\mathbf{k}}|/E)}{1-v+2|\vec{\mathbf{k}}|/E}\right]. \quad \text{(B20)}$$

Here E and v are the energy and velocity of the jet.

By using relations (B19) and (B20), Eq. (B17) finally reduces to

$$\Delta E_{el} = \frac{C_Rg^4}{2\pi^4}\int_0^\infty n_{eq}(|\vec{\mathbf{k}}|)d|\vec{\mathbf{k}}|\ \left(\int_0^{|\vec{\mathbf{k}}|}|\vec{\mathbf{q}}|d|\vec{\mathbf{q}}|\int_{-|\vec{\mathbf{q}}|}^{|\vec{\mathbf{q}}|}\omega d\omega + \int_{|\vec{\mathbf{k}}|}^{|\vec{\mathbf{q}}|_{\max}}|\vec{\mathbf{q}}|d|\vec{\mathbf{q}}|\int_{|\vec{\mathbf{q}}|-2|\vec{\mathbf{k}}|}^{|\vec{\mathbf{q}}|}\omega d\omega\right) \times\left(|\Delta_L(q)|^2\frac{(2|\vec{\mathbf{k}}|+\omega)^2-|\vec{\mathbf{q}}|^2}{2}\mathcal{J}_1 + |\Delta_T(q)|^2\frac{(|\vec{\mathbf{q}}|^2-\omega^2)((2|\vec{\mathbf{k}}|+\omega)^2+|\vec{\mathbf{q}}|^2)}{4|\vec{\mathbf{q}}|^4} \times\left[(v^2|\vec{\mathbf{q}}|^2-\omega^2)\mathcal{J}_1+2\omega\mathcal{J}_2-\mathcal{J}_3\right]\right), \quad \text{(B21)}$$

where $|\vec{\mathbf{q}}|_{\max}$ is given in Eq. (B20).

Large L limit

In this subsection we will consider the large L limit case, and compute the collisional energy loss per unit length. To do that we multiply both sides of the Eq. (B17) by $\frac{2v}{\pi L}$, i.e.,

$$\frac{2v}{\pi L}\Delta E_{el} = \frac{C_Rg^4}{2\pi^4}\int n_{eq}(|\vec{\mathbf{k}}|)d|\vec{\mathbf{k}}|\ |\vec{\mathbf{q}}|d|\vec{\mathbf{q}}|\ \omega d\omega \times\left(|\Delta_L(q)|^2\frac{(2|\vec{\mathbf{k}}|+\omega)^2-|\vec{\mathbf{q}}|^2}{2}\frac{2v}{\pi L}\mathcal{J}_1 + |\Delta_T(q)|^2 \times\frac{(|\vec{\mathbf{q}}|^2-\omega^2)((2|\vec{\mathbf{k}}|+\omega)^2+|\vec{\mathbf{q}}|^2)}{4|\vec{\mathbf{q}}|^4} \times\left[(v^2|\vec{\mathbf{q}}|^2-\omega^2)\frac{2v}{\pi L}\mathcal{J}_1 + 2\omega\frac{2v}{\pi L}\mathcal{J}_2-\frac{2v}{\pi L}\mathcal{J}_3\right]\right). \quad \text{(B22)}$$

To compute $\frac{2v}{\pi L}\mathcal{J}_{1,2,3}$ in the limit when $L\to\infty$ we will use the following expression:

$$\frac{2v}{\pi L}\frac{\sin\left[(\omega-\vec{\mathbf{v}}\cdot\vec{\mathbf{q}})\frac{L}{2v}\right]^2}{(\omega-\vec{\mathbf{v}}\cdot\vec{\mathbf{q}})^2}\xrightarrow{L\to\infty}\delta(\omega-\vec{\mathbf{v}}\cdot\vec{\mathbf{q}}). \quad \text{(B23)}$$

Then,

$$\frac{2v}{\pi L}\mathcal{J}_1 \xrightarrow{L\to\infty} \int \frac{d\Omega}{4\pi}\delta(\omega-\vec{\mathbf{v}}\cdot\vec{\mathbf{q}}) = \frac{1}{2v|\vec{\mathbf{q}}|}\Theta\left(v^2|\vec{\mathbf{q}}|^2-\omega^2\right), \tag{B24}$$

$$\frac{2v}{\pi L}\mathcal{J}_2 \xrightarrow{L\to\infty} \int \frac{d\Omega}{4\pi}\delta(\omega-\vec{\mathbf{v}}\cdot\vec{\mathbf{q}})(\omega-\vec{\mathbf{v}}\cdot\vec{\mathbf{q}}) = 0 \tag{B25}$$

and

$$\frac{2v}{\pi L}\mathcal{J}_3 \xrightarrow{L\to\infty} \int \frac{d\Omega}{4\pi}\delta(\omega-\vec{\mathbf{v}}\cdot\vec{\mathbf{q}})(\omega-\vec{\mathbf{v}}\cdot\vec{\mathbf{q}})^2 = 0, \tag{B26}$$

leading to

$$\begin{aligned}\frac{2v}{\pi L}\Delta E_{el} = \frac{C_R g^4}{2\pi^4}\int n_{eq}(|\vec{\mathbf{k}}|)d|\vec{\mathbf{k}}|\ |\vec{\mathbf{q}}|d|\vec{\mathbf{q}}|\ \omega d\omega \\ \times \frac{1}{2v|\vec{\mathbf{q}}|}\Theta(v^2|\vec{\mathbf{q}}|^2-\omega^2) \\ \times \left(|\Delta_L(q)|^2\frac{(2|\vec{\mathbf{k}}|+\omega)^2-|\vec{\mathbf{q}}|^2}{2}+|\Delta_T(q)|^2\right. \\ \left.\times \frac{(|\vec{\mathbf{q}}|^2-\omega^2)((2|\vec{\mathbf{k}}|+\omega)^2+|\vec{\mathbf{q}}|^2)}{4|\vec{\mathbf{q}}|^4}\right. \\ \left.\times (v^2|\vec{\mathbf{q}}|^2-\omega^2)\right).\end{aligned} \tag{B27}$$

Therefore, by using relations (B19), (B20) and $v^2|\vec{\mathbf{q}}|^2 > \omega^2$, the collisional energy loss per unit length in an infinite size QCD medium reduces to the following expression ($C_R = 4/3$)

$$\begin{aligned}\frac{dE_{el}}{dL} = \frac{g^4}{6v^2\pi^3}\int_0^\infty n_{eq}(|\vec{\mathbf{k}}|)d|\vec{\mathbf{k}}|\ \left(\int_0^{2|\vec{\mathbf{k}}|/(1+v)} d|\vec{\mathbf{q}}|\right. \\ \times \int_{-v|\vec{\mathbf{q}}|}^{v|\vec{\mathbf{q}}|}\omega d\omega + \int_{2|\vec{\mathbf{k}}|/(1+v)}^{|\vec{\mathbf{q}}|_{\max}} d|\vec{\mathbf{q}}|\int_{|\vec{\mathbf{q}}|-2|\vec{\mathbf{k}}|}^{v|\vec{\mathbf{q}}|}\omega d\omega\Big) \\ \times \left(|\Delta_L(q)|^2\frac{(2|\vec{\mathbf{k}}|+\omega)^2-|\vec{\mathbf{q}}|^2}{2}+|\Delta_T(q)|^2\right. \\ \left.\times \frac{(|\vec{\mathbf{q}}|^2-\omega^2)((2|\vec{\mathbf{k}}|+\omega)^2+|\vec{\mathbf{q}}|^2)}{4|\vec{\mathbf{q}}|^4}(v^2|\vec{\mathbf{q}}|^2-\omega^2)\right).\end{aligned} \tag{B28}$$

[1] M. Gyulassy, Lect. Notes Phys. **583**, 37 (2002).
[2] M. Gyulassy and M. Plümer, Nucl. Phys. **A527**, 641 (1991).
[3] M. Gyulassy, M. Plümer, M. Thoma, and X. N. Wang, Nucl. Phys. **A538**, 37C (1992); X. N. Wang and M. Gyulassy, Phys. Rev. Lett. **68**, 1480 (1992).
[4] M. Gyulassy, I. Vitev, X. N. Wang, and B. W. Zhang, *Quark Gluon Plasma 3*, edited by R. C. Hwa and X. N. Wang (World Scientific, Singapore, 2003), p. 123 (nucl-th/0302077).
[5] R. Baier, Yu. L. Dokshitzer, A. J. Mueller, and D. Schiff, Phys. Rev. C **58**, 1706 (1998).
[6] R. Baier, D. Schiff, and B. G. Zakharov, Ann. Rev. Nucl. Part Sci. **50**, 37 (2000).
[7] A. Kovner and U. A. Wiedemann, in Ref. [4], p. 192 (hep-ph/0304151).
[8] S. S. Adler *et al*. (PHENIX Collaboration), Phys. Rev. Lett. **96**, 032301 (2006); Y. Akiba (PHENIX Collaboration), Nucl. Phys. **A774**, 403 (2006).
[9] J. Bielcik (STAR Collaboration), Nucl. Phys. **A774**, 697 (2006); X. Dong (STAR Collaboration), *ibid*. **A774**, 343 (2006).
[10] M. Djordjevic, M. Gyulassy, R. Vogt, and S. Wicks, Phys. Lett. **B632**, 81 (2006).
[11] M. G. Mustafa, Phys. Rev. C **72**, 014905 (2005); M. G. Mustafa and M. H. Thoma, Acta Phys. Hung. A **22**, 93 (2005).
[12] A. K. Dutt-Mazumder, J. Alam, P. Roy, and B. Sinha, Phys. Rev. D **71**, 094016 (2005).
[13] J. D. Bjorken, FERMILAB-PUB-82-059-THY (unpublished).
[14] M. H. Thoma and M. Gyulassy, Nucl. Phys. **B351**, 491 (1991).
[15] E. Braaten and M. H. Thoma, Phys. Rev. D **44**, R2625 (1991).
[16] X. N. Wang, M. Gyulassy, and M. Plümer, Phys. Rev. D **51**, 3436 (1995).
[17] M. G. Mustafa, D. Pal, D. K., and M. Thoma, Phys. Lett. **B428**, 234 (1998).
[18] Z. W. Lin, R. Vogt, and X. N. Wang, Phys. Rev. C **57**, 899 (1998).
[19] S. Wicks, W. Horowitz, M. Djordjevic, and M. Gyulassy, arXiv:nucl-th/0512076 (2006).
[20] S. Peigne, P. B. Gossiaux, and T. Gousset, J. High Energy Phys. 04 (2006) 011.
[21] M. Djordjevic and M. Gyulassy, Phys. Rev. C **68**, 034914 (2003).
[22] M. Djordjevic and M. Gyulassy, Phys. Lett. **B560**, 37 (2003).
[23] M. Djordjevic, Phys. Rev. C **73**, 044912 (2006).
[24] E. Braaten and M. H. Thoma, Phys. Rev. D **44**, 1298 (1991).
[25] G. Baym, H. Monien, C. J. Pethick, and D. G. Ravenhall, Phys. Rev. Lett. **64**, 1867 (1990).
[26] B. G. Zakharov, JETP Lett. **76**, 201 (2002).
[27] M. Gyulassy, P. Levai, and I. Vitev, Nucl. Phys. **B594**, 371 (2001).
[28] O. K. Kalashnikov and V. V. Klimov, Sov. J. Nucl. Phys. **31**, 699 (1980).
[29] V. V. Klimov, Sov. Phys. JETP **55**, 199 (1982).
[30] R. D. Pisarski, Physica A **158**, 146 (1989).
[31] A. Rebhan, Lect. Notes Phys. **583**, 161 (2002); hep-ph/0111341.
[32] A. V. Selikhov, M. Gyulassy, Phys. Lett. **B316**, 373 (1993); Phys. Rev. C **49**, 1726 (1994).
[33] M. Djordjevic, M. Gyulassy, and S. Wicks, Phys. Rev. Lett. **94**, 112301 (2005).
[34] P. Romatschke and M. Strickland, Phys. Rev. D **71**, 125008 (2005).
[35] M. Djordjevic and M. Gyulassy, Nucl. Phys. **A733**, 265 (2004).
[36] A. Peshier, arXiv:hep-ph/0605294 (2006).
[37] X. N. Wang, arXiv:nucl-th/0604040 (2006).
[38] A. Adil, M. Gyulassy, W. A. Horowitz, and S. Wicks, arXiv:nucl-th/0606010 (2006).